Ionic and electronic dark decay of holograms in $LiNbO_3$:Fe crystals

Yunping Yang[a)]
Department of Electrical Engineering, California Institute of Technology, Pasadena, California 91125

Ingo Nee and Karsten Buse[b)]
Fachbereich Physik, Universität Osnabrück, D-49069 Osnabrück, Germany

Demetri Psaltis
Department of Electrical Engineering, California Institute of Technology, Pasadena, California 91125

(Received 21 November 2000; accepted for publication 27 April 2001)

The lifetimes of nonfixed holograms in $LiNbO_3$:Fe crystals with doping levels of 0.05, 0.138, and 0.25 wt % Fe_2O_3 have been measured in the temperature range from 30 to 180 °C. The time constants of the dark decay of holograms stored in crystals with doping levels of 0.05 and 0.25 wt % Fe_2O_3 obey an Arrhenius-type dependence on absolute temperature T, but yield two activation energies: 1.0 and 0.28 eV, respectively. For these crystals, two different dark decay mechanisms are prevailing, one of which is identified as proton compensation and the other is due to electron tunneling between sites of Fe^{2+} and Fe^{3+}. The dark decay of holograms stored in crystals with the doping level of 0.138 wt % Fe_2O_3 is the result of a combination of both effects. © *2001 American Institute of Physics.* [DOI: 10.1063/1.1380247]

Photorefractive $LiNbO_3$:Fe crystals have been of intense interest in the fields of holographic data storage[1–4] and narrow-band wavelength filters for optical telecommunications.[5–8] Photorefractive volume phase gratings can be produced in electro-optic materials by redistribution of excited carriers in the presence of light. One of the most important issues is the dark decay due to the dark conductivity. The time constant of the dark decay τ is defined as the time until the grating strength decays in the dark to $1/e$ of the original value and is related to the dark conductivity σ_d as $\tau = \epsilon_0 \epsilon / \sigma_d$, where ϵ is the dielectric constant of lithium niobate. Lifetimes of nonfixed holograms in $LiNbO_3$:Fe crystals vary between a few minutes and one year.[9–11] These lifetimes are generally too short for practical applications. In order to improve the lifetimes, a good understanding of the origins of the dark decay is needed.

Recently, it has been found that in the dark and at room temperature electron tunneling between iron sites occurs in highly doped crystals.[11] It is generally accepted that for the temperature range between 150 and 200 °C the proton conductivity is enlarged by several orders of magnitude compared to that at room temperature. This behavior is used for thermal fixing.[12] For temperatures higher than 200 °C, excitation of electrons into the conduction band is supposed to be the main process.[13] Up to now, the thermal activation energy of the electron tunneling process is unknown. A study of the process at and close to room temperature is of special importance. Lifetime estimates of holograms stored in lithium niobate are frequently based on extrapolation of high-temperature data. This is risky because proper thermal activation energies must be used. In this work, the dark decay of holographic gratings in $LiNbO_3$:Fe crystals with different doping levels in the temperature range from 30 to 180 °C has been measured. From the experimental data, two different activation energies have been extracted, namely, 1.0 and 0.28 eV. These two activation energies are identified to correspond to different dark decay mechanisms: proton compensation and electron tunneling,[11] respectively.

Congruently melting $LiNbO_3$:Fe samples are used, two of which have a doping level of 0.05 wt % Fe_2O_3, two with a doping level of 0.138 wt % Fe_2O_3, and one doped with 0.25 wt % Fe_2O_3. Table I summarizes some parameters of these samples. All these crystals were x cut and polished to optical quality. Thermal annealing in various atmospheres is used to achieve desired oxidation states and proton concentrations. The shape of the absorption spectra is the same for all crystals used, i.e., we avoid too strong reduction that generates, e.g., polaron and bipolaron bands. Thus, the Fe^{2+} concentration $c_{Fe^{2+}}$ can be calculated from absorption measurements.[14] Because iron occurs only in the valence states 2+ and 3+, the concentration of Fe^{3+} is determined by subtracting $c_{Fe^{2+}}$ from the entire iron concentration c_{Fe}. The absorption coefficient at the maximum of the OH^- absorption at 2870 nm is used to calculate the proton concentration.[15]

The crystals were placed on a heatable plate whose temperature was controlled within 0.1 °C accuracy. An argon-ion laser beam with a wavelength of 514 nm was used in all of the experiments to record the holograms. The laser beam was split into two equal-intensity extraordinarily polarized beams

TABLE I. Summary of the parameters of the samples.

Sample	Doping level (wt % Fe_2O_3)	Oxidation state $c_{Fe_{2+}}/c_{Fe_{3+}}$	Comments
S1	0.05	0.05	Proton enriched
S2	0.05	0.21	Proton reduced
S3	0.25	0.10	Proton reduced
S4	0.138	0.03	Proton enriched
S5	0.138	0.03	Proton reduced

a)Electronic mail: yunping@optics.caltech.edu
b)Present address: Physikalisches Institut, Universität Bonn, Wegelerstraße 8, D-53115 Bonn, Germany.

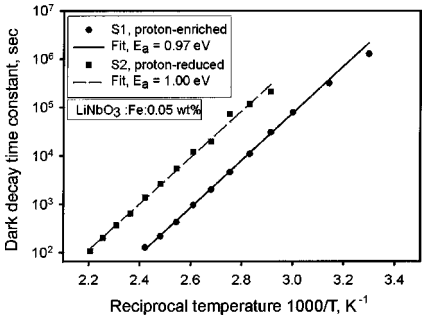

FIG. 1. Arrhenius plot of the dark decay time constants of holograms stored in $LiNbO_3$:Fe crystals with a doping level of 0.05 wt % Fe_2O_3, sample S1: proton enriched and sample S2: proton reduced.

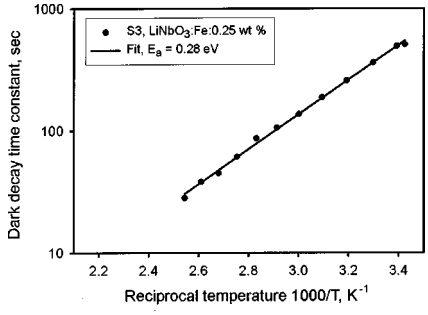

FIG. 2. Arrhenius plot of dark decay time constants of holograms in $LiNbO_3$:Fe crystals with a doping level of 0.25 wt % Fe_2O_3, sample S3: proton reduced.

that were expanded to cover the whole crystal during recording. All recorded holograms had a grating period of 1.3 μm and were written with the grating vector oriented along the c axis. Recording was always performed at room temperature. Afterwards, the crystals were heated to a certain temperature in the dark and a weak laser beam of 514 nm was used to monitor the holographic diffraction efficiency. The weak readout light illuminated the crystal only from time to time, and the intervals between two measurements were long enough to keep the erasure of the holograms by the probing beam negligible. After each experiment the crystal was heated to 230 °C and kept at this temperature under uniform illumination for about 45 min to erase the gratings completely.

The two crystals with the doping level of 0.05 wt % Fe_2O_3, S1 and S2, were cut from the same boule. Sample S1 was proton enriched by suitable annealing treatment while sample S2 was proton reduced. The proton concentrations of samples S1 and S2 were 5.5×10^{24} and $3.1\times10^{23}\,m^{-3}$, respectively. Figure 1 shows the measured dark decay time constants of these two crystals. The time constants of both crystals obey an Arrhenius-type dependence on the absolute temperature T, $\tau=\tau_0\exp(E_a/k_BT)$, where τ_0 is a pre-exponential factor, k_B is the Boltzmann constant, and E_a is the activation energy. There are several justifications that the dark decay in these two crystals is dominated by proton compensation of the electrical space-charge field. The activation energies obtained for samples S1 and S2 are almost the same, 0.97 and 1.0 eV, respectively, and close to the proton activation energies reported in the literature.[16,17] The ratio of the fitted pre-exponential factors for samples S2 and S1 is 18.3, which is, as it should be, almost equal to the reciprocal ratio of the proton concentrations of these two samples, namely, 17.7. Noting the fact that sample S2 is reduced much more than sample S1, but the preexponential factor of sample S1 is even less than that of sample S2, we can rule out the possibility that the dark decay is related to the iron doping and electronic band transport since the time constant of the dark decay due to band transport should be inversely proportional to the oxidation state $c_{Fe^{2+}}/c_{Fe^{3+}}$. We would like to emphasize the large range of temperatures used. Measurements were taken from room temperature up to 180 °C.

Figure 2 shows the measured dark decay time constants for sample S3, a $LiNbO_3$:Fe crystal doped with 0.25 wt % Fe_2O_3. Although the plot is still Arrhenius-like, the activation energy, 0.28 eV, is much smaller than that of samples S1 and S2. Obviously, there is a mechanism other than proton compensation dominating the dark decay. This mechanism has been identified as electron tunneling between sites of Fe^{2+} and Fe^{3+}.[11] It is interesting that just increasing the doping level by a factor of 5 yields a totally different dark decay mechanism. The dependence of the dark decay time constant on the doping level is exponential. The pre-exponential factor of Arrhenius law is proportional to $[c_{Fe^{2+}}c_{Fe^{3+}}/(c_{Fe^{2+}}+c_{Fe^{3+}})]\exp[a(c_{Fe})^{1/3}]$ for electron tunneling.[11] This type of dark decay limits the highest practical doping level for $LiNbO_3$:Fe crystals.

For $LiNbO_3$:Fe crystals with low doping levels, proton compensation dominates the dark decay, while for those with a doping level as high as 0.25 wt % Fe_2O_3, the dominant mechanism is electron tunneling. It is reasonable to expect both these two effects to be present in some crystals with doping levels between 0.05 and 0.25 wt % Fe_2O_3. Figure 3 shows exactly the picture that we expect. Two crystals, S4 and S5, each with a doping level of 0.138 wt % Fe_2O_3 have been used. Both of these crystals were cut from the same boule. Sample S4 was proton enriched and sample S5 was proton reduced with proton concentrations 5.6×10^{24} and $3.0\times10^{23}\,m^{-3}$, respectively. The oxidation states in these two crystals are more or less the same. Since the activation energy of proton compensation is much larger than that of electron tunneling, the dependence of the time constant on the absolute temperature is stronger for proton compensation. At high temperatures, the proton compensation plays a larger role; thus, we see the difference between these two crystals in the high-temperature range due to the different proton contents. At low temperatures, e.g., room temperature, the effect of electron tunneling prevails. Since the crys-

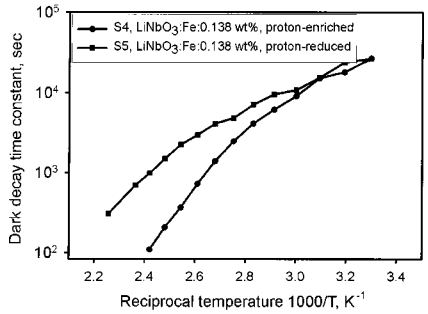

FIG. 3. Dark decay time constant vs reciprocal temperature in $LiNbO_3$:Fe crystals with a doping level of 0.138 wt % Fe_2O_3, sample S4: proton enriched and sample S5: proton reduced.

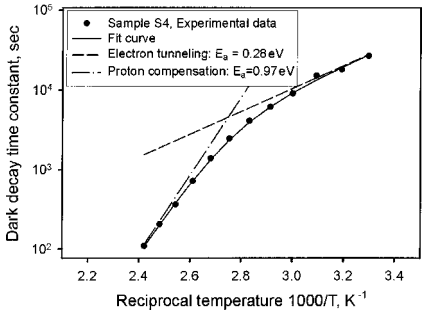

FIG. 4. Dark decay time constant vs reciprocal temperature of sample S4. The solid line is a fit of equation $\tau_d=[\tau_p(T)\tau_e(T)]/[\tau_p(T)+\tau_e(T)]$ to the experimental data.

tals have the same doping level and the same oxidation state, we should not see much disparity of the dark decay between samples S4 and S5 at low temperatures, which is exactly what Fig. 3 shows. Fitting the data in the low-temperature range to an Arrhenius law yields an activation energy close to what we got from Fig. 2, which means the dominant dark decay mechanism at room temperature in these two crystals is the same as that in crystal S3.

In crystals where both proton compensation and electron tunneling matter, the dark conductivity σ_d should be: $\sigma_d=\sigma_p+\sigma_e$, where σ_p and σ_e are dark conductivity due to proton compensation and electron tunneling, respectively. The decay time constant τ is related to the conductivity σ_d as $\tau=\epsilon_0\epsilon/\sigma_d$, so we have $\tau_d=[\tau_p(T)\tau_e(T)]/[\tau_p(T)+\tau_e(T)]$, where $\tau_p(T)=\tau_{0p}\exp(E_{ap}/k_BT)$ and $\tau_e(T)=\tau_{0e}\exp(E_{ae}/k_BT)$. We fit this equation to the experimental data obtained with sample S4 using a proton compensation activation energy of 0.97 eV and an electron tunneling activation energy of 0.28 eV. The result is shown in Fig. 4, which is, as we can see, very good. We also did the fitting with the data obtained with sample S5. From the fitted pre-exponential factors of the proton compensation we estimate that the ratio of the proton concentrations of samples S4 and S5 is about 22, which agrees very well with the factor 19 determined by absorption measurements.

In conclusion, two mechanisms of the dark decay, proton compensation and electron tunneling with activation energies of 1.0 and 0.28 eV, respectively, have been identified. In crystals with doping levels less than 0.05 wt % Fe_2O_3, proton compensation dominates the dark decay and extrapolation of lifetimes by an Arrhenius law to room temperature is valid. The time constant of this type of dark decay is inversely proportional to the proton concentration. For crystals with doping levels as high as 0.25 wt % Fe_2O_3, electron tunneling dominates the dark decay. This type of dark decay also limits the highest practical doping level in $LiNbO_3$:Fe crystals in, e.g., holographic storage systems and optical narrow-band wavelength filters. For crystals with doping levels between 0.05 and 0.25 wt % Fe_2O_3, both proton compensation and electron tunneling contribute significantly to the dark decay, and the single Arrhenius law does not hold anymore with a single activation energy. Caution is required in extrapolating the lifetime of room-temperature holograms from the experimental data obtained at high temperatures.

This effort was sponsored by NSF, Center for Neuromorphic Systems Engineering ERC, DARPA, and Volkswagen-Stiftung. The authors thank the NSF and the DAAD for sponsoring the U.S.–German collaboration.

[1] D. Psaltis and F. Mok, Sci. Am. **273**, 70 (1995).
[2] I. McMichael, W. Christian, D. Pletcher, T. Y. Chang, and J. H. Hong, Appl. Opt. **35**, 2375 (1996).
[3] R. M. Shelby, J. A. Hoffnagle, G. W. Burr, C. M. Jefferson, M.-P. Bernal, H. Coufal, R. K. Grygier, H. Günther, R. M. Macfarlane, and G. T. Sincerbox, Opt. Lett. **22**, 1509 (1997).
[4] J.-J. P. Drolet, E. Chuang, G. Barbastathis, and D. Psaltis, Opt. Lett. **22**, 552 (1997).
[5] V. Leyva, G. A. Rakuljic, and B. O'Conner, Appl. Phys. Lett. **65**, 1079 (1994).
[6] R. Müller, M. T. Santos, L. Arizmendi, and J. M. Cabrera, J. Phys. D **27**, 241 (1994).
[7] S. Breer and K. Buse, Appl. Phys. B: Lasers Opt. **66**, 339 (1999).
[8] S. Breer, H. Vogt, I. Nee, and K. Buse, Electron. Lett. **34**, 2419 (1998).
[9] E. Krätzig and R. Orlowski, Appl. Phys. **15**, 133 (1978).
[10] D. Kip, J. Hukriede, and E. Krätzig, Phys. Status Solidi A **168**, R3 (1998).
[11] I. Nee, M. Müller, K. Buse, and E. Krätzig, J. Appl. Phys. **88**, 4282 (2000).
[12] J. J. Amodei and D. L. Staebler, Appl. Phys. Lett. **18**, 540 (1971).
[13] B. I. Sturman, M. Carrascosa, F. Agullo-Lopez, and J. Limeres, Phys. Rev. B **57**, 12792 (1998).
[14] H. Kurz, E. Krätzig, W. Keune, H. Engelman, U. Gonser, B. Dischler, and A. Räuber, Appl. Phys. **12**, 355 (1977).
[15] S. Kapphan and A. Breitkopf, Phys. Status Solidi A **133**, 159 (1992).
[16] D. L. Staebler and J. J. Amodei, Ferroelectrics **3**, 107 (1972).
[17] L. Arizmendi, P. D. Townsend, M. Carrascosa, J. Baquedano, and J. M. Cabrera, J. Phys.: Condens. Matter **3**, 5399 (1991).